Analytical Methods

Accepted Manuscript

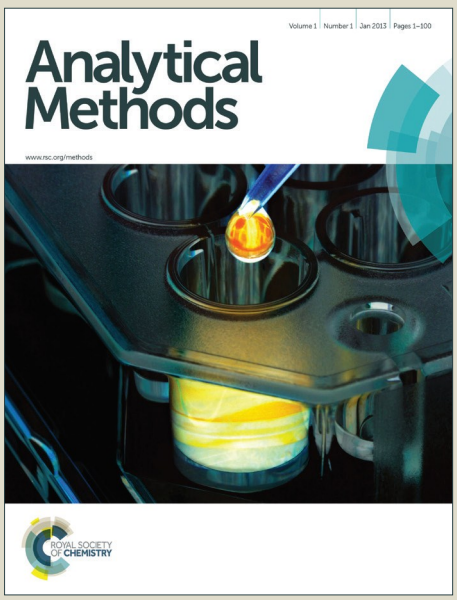

This is an *Accepted Manuscript*, which has been through the Royal Society of Chemistry peer review process and has been accepted for publication.

Accepted Manuscripts are published online shortly after acceptance, before technical editing, formatting and proof reading. Using this free service, authors can make their results available to the community, in citable form, before we publish the edited article. We will replace this *Accepted Manuscript* with the edited and formatted *Advance Article* as soon as it is available.

You can find more information about *Accepted Manuscripts* in the Information for Authors.

Please note that technical editing may introduce minor changes to the text and/or graphics, which may alter content. The journal's standard Terms & Conditions and the Ethical guidelines still apply. In no event shall the Royal Society of Chemistry be held responsible for any errors or omissions in this *Accepted Manuscript* or any consequences arising from the use of any information it contains.

ROYAL SOCIETY OF CHEMISTRY

www.rsc.org/methods

Estimation of Methylglyoxal in Cow Milk – An Accurate Electrochemical Response Time based Approach

[1,2,3]Bhat Lakshmishri Ramachandra, [1,3,4]Srinivasan Vedantham, [1,3,4]Uma Maheswari Krishnan [1,2,3]Noel Nesakumar and [1,2,3]John Bosco Balaguru Rayappan*

[1]*Nanosensors Lab, SASTRA University, Thanjavur 613 401, Tamil Nadu, India*

[2]*School of Electrical & Electronics Engineering, SASTRA University, Thanjavur 613 401, Tamil Nadu, India*

[3]*Centre for Nanotechnology & Advanced Biomaterials, SASTRA University, Thanjavur 613 401, Tamil Nadu, India*

[4]*School of Chemical and Biotechnology, SASTRA University, Thanjavur 613 401, Tamil Nadu, India*

***Corresponding Author**

Prof. John Bosco Balaguru Rayappan

Centre for Nanotechnology & Advanced Biomaterials (CeNTAB) &

School of Electrical & Electronics Engineering

SASTRA University

Thanjavur – 613 401

India.

Ph: +91 4362 264 101; Ext: 255

Fax: +91 4362 264120

Email: rjbosco@ece.sastra.edu

Abstract

Cow milk contains carbohydrates that are prone for methylglyoxal (MG) production which plays a major role in chronic complications of diabetes. In this context, an electrochemical biosensor based on glyoxalase 1 (GLO 1) modified platinum electrode (Pt) with ceria nano-interface (CeO_2) was developed. Fabricated Pt/CeO_2/GLO 1/Chitosan nano-bioelectrode reduced MG and hemithioacetal at -0.771 and -0.558 V respectively in the presence of glutathione (GSH). Michaelis-Menten and Hill models were employed for estimation of response time. Accuracy of these models was validated by calculating relative prediction error. Only the modified Hill model showed best results in validation. The sensitivity of Pt/CeO_2/GLO 1/Chitosan nano-bioelectrode at -0.771 V was 2.868 μA μM^{-1} over a linear range between 5 and 50 μM, a detection limit of 2.14 nM, a quantification limit of 7.12 nM and a response time of less than 39 s. The fabricated electrode demonstrated to be highly reproducible with relative standard deviation of 1.02% for 10 successive amperometric calibrations. It also showed good recovery (99.21-101.72%), thus providing a promising tool for analysis of MG in cow milk.

Keywords: Response time; Methylglyoxal; Electrochemical biosensor; Ceria nano-interface; Quantification; Cow milk

1. Introduction

Methylglyoxal (MG), a precursor of advanced glycation end products (AGE)[1], plays a major role in chronic complications of diabetes[2–4]. It is present in cow milk[5] and cooked foods especially foods prepared from frying, searing, roasting, broiling and grilling[6]. Hence rapid and portable analytical equipment is needed for the determination of MG especially in cow milk since it is being consumed by all age groups.

The conventional methods used for the detection of MG are high performance liquid chromatography (HPLC), gas chromatography[7], GC-MS[8], ion pair chromatography, MEKC[9], capillary electrophoresis and enzyme-linked immunosorbent assay (ELISA), which are time consuming and expensive[10–13]. Electrochemical biosensors have been proposed for methylglyoxal detection, which are simple, highly selective, low-cost, rapid and portable[10–15]. Various nanoparticles such as zinc oxide (ZnO) nanosepals and flakes, platinum (Pt) and single wall carbon nanotube (SWCNT) have been employed as the effective immobilization matrices for the development of highly sensitive MG biosensor[10–13]. Among them, ZnO nanosepals and flakes were used as interfaces for glyoxalase1 (GLO 1) immobilization towards the detection of MG in blood and grilled chicken respectively. Whereas, Pt and SWCNT play the role of glutathione (GSH), which involved in direct catalysis of MG to hemithioacetal. Though the function of GSH could be mimicked, the inability of these nanomaterials for specific and selective detection of MG makes them inferior. Moreover, the three peaks arouse due to the formation of glutathione disulfide, hemithioacetal and S-D-lactoylglutathione have been not reported in any of these works. In order to overcome these drawbacks, GLO 1 enzyme was used to catalyze the MG reduction reaction in which GLO 1 showed high specificity towards MG[12,13].

Like ZnO nanoparticles, cerium oxide (CeO_2) nanoparticles have attracted researchers in the fabrication of electrochemical biosensors because of their good biocompatibility[16],

catalytic property[17], electron transfer rate and large surface area to volume ratio[16]. CeO_2 nanoparticles have an isoelectric point of 9.2[18], which can immobilize GLO 1 enzyme of low isoelectric point of pI = 4.8 by electrostatic attraction[12,13,19] and prevent leaching of enzyme. Although, in all these works recovery studies were performed with real time sample analysis in wine, beer, etc., response time – the analytical tool for measuring the rapidness of the system was never reported. Till date, the electroanalytical techniques used for the measurement of MG are cyclic voltammetry (CV), linear sweep voltammetry (LSV) and square wave voltammetry (SWV). All of them are incompetent for response time measurement and amperometry would be a potential candidate.

Conventionally, averaging of the response in the linear range frame is the method mostly implemented in sensors which lead to erroneous results. In fact, response time would vary with respect to each substrate concentration. Michaelis-Menten and Hill models provide a platform for detailed study of concentration variation with response time. Also these models are commonly used in enzyme kinetics due to their hyperbolic and sigmoidal nature resembling the amperometric i-t curve. In this work, Pt/CeO_2/GLO 1/Chitosan nano-bioelectrode has been fabricated to detect MG in cow milk using amperometry and to study the effect of response time relating to the concentration variation.

2. Materials and methods

2.1. Materials

Human glyoxalase1 (Molecular weight: 20.7 kDa, ≥90% (SDS-PAGE)) and methylglyoxal (Molecular weight: 69.49 g M^{-1}) were purchased from Sigma-Aldrich, USA. L-Glutathione-reduced (GSH, Molecular weight: 307.32 g M^{-1}) was purchased from Hi-Media, India. All the other chemicals such as chitosan, sodium hydroxide pellets purified, glucose, ascorbic acid, sucrose, lactic acid, urea, monobasic sodium phosphate and dibasic sodium phosphate were purchased from Merck India Ltd., India. Nickel acetate, zinc acetate

and cupric acetate were purchased from Thermo Fisher Scientific Pvt. Ltd., India. Cadmium acetate was purchased from Loba Chemie Pvt. Ltd., Mumbai, India. All the reagents and solutions were prepared using double de-ionized water (Aqua purification systems, India).

2.2. Synthesis of CeO_2 nanoparticles

0.25 M cerium nitrate hexahydrate was prepared, to which 0.75 M of NaOH was added and stirred for 14 h at room temperature to obtain a yellow coloured precipitate. Then, the precipitate was centrifuged at 8500 rpm for 30 min. Later, the pellets were kept in hot air oven at 423 K for 6 h, which yielded CeO_2 particles in dried form. Finally, the powdered sample was annealed at 523 K for 6 h.

2.3. Fabrication of Pt/CeO_2/GLO 1/Chitosan nano-bioelectrode

200 µL of chitosan solution was added to 1 mg of CeO_2 nanoparticles and the resulting mixture was sonicated for 15 min. Later, 10 µL of GLO 1 enzyme was added to the above mixture, which was further sonicated for 2 min. Finally, 3 µL of the solution containing CeO_2-GLO 1-chitosan mixture was taken and casted on the surface of Pt working electrode. After drying it for 5 h at room temperature, the Pt/CeO_2/GLO 1/Chitosan nano-bioelectrode was employed for electrochemical measurements.

2.4. Instrumentation and characterization

The surface morphology and size distribution of CeO_2 particles were studied using Field Emission Scanning Electron Microscopy (FE-SEM, Model JSM 6701F, JEOL, Japan) and Image J 1.48 q software respectively. An electrochemical analyzer (CHI 600C, CH Instruments, Inc., USA) was employed with the modified Pt (Pt/GLO 1/Chitosan and Pt/CeO_2/GLO 1/Chitosan) as the working electrode (3 mm diameter, CHI 104, CH Instruments, Inc., USA), Ag/AgCl (CHI 111, CH Instruments, Inc., USA) as reference electrode and Pt wire (0.5 mm diameter, CHI 115, CH Instruments, Inc., USA) as counter

electrode to record electrochemical response. All electrochemical analyses were carried out at room temperature in 0.1 M PBS (pH 7.4).

2.5. Modified Michaelis-Menten model for the determination of response time

Amperometric curve for glyoxalase1 (GLO 1) reaction showing the relation between the methylglyoxal concentration ($[MG]$) and the current density (J) can be written as

$$J = \frac{J_{max}[MG]}{K_M + [MG]} \quad \text{--- (1)}$$

where, J_{max} is the maximum current density and K_M is the MG concentration at which the current density is half of J_{max}. Since the amperometric i-t curve of MG biosensor shows hyperbolic relationship between current density and time, the MG concentration in Eq. (1) is replaced with time (t),

$$J = \frac{J_{max}t}{t_{50\%} + t} \quad \text{--- (2)}$$

Since the minimum and maximum current densities are the lower and upper limits of amperometric i-t curve, modified Michaelis-Menten model with J_{min} as an intercept was included.

$$J = \frac{J_{max}t}{t_{50\%} + t} + J_{min} \quad \text{--- (3)}$$

It is expected that $t_{50\%}$ is equal to t, when $J = \frac{J_{max} - J_{min}}{2}$. However, the Eq. (3) gives $J = \frac{J_{max} + 2J_{min}}{2}$ when $t = t_{50\%}$, which may lead to inaccurate estimation of $t_{50\%}$. Hence for the precise estimation of $t_{50\%}$ and J_{max}, the Eq. (3) is rewritten as,

$$J = (J_{max} - J_{min})\frac{t}{t_{50\%} + t} + J_{min},\ t_{min} \le t \le t_{max} \quad \text{--- (4)}$$

where, $t_{50\%}$is the 50% response time at $J = \frac{J_{max} - J_{min}}{2}$. At $t = 0$, $J = J_{min}$. Similarly, at $t = t_{max}$, $J = (J_{max} - J_{min})\frac{t_{max}}{t_{50\%} + t_{max}} + J_{min}$. Since response time[20] is the time needed for the Pt/CeO_2/GLO 1/Chitosan nano-bioelectrode to reach 90, 95 and 99% of its stable value,

the same at 90 ($t_{90\%}$), 95 ($t_{95\%}$) and 99% ($t_{99\%}$) of the steady state current density value was calculated using Eq. (4).

In order to evaluate the 90% response time when the amperometric current density response is 90% of its steady state value, $J = 90\%J_{max}$ is substituted in the Eq. (4).

$$0.90J_{max} = (J_{max} - J_{min})\frac{t_{90\%}}{t_{50\%} + t_{90\%}} + J_{min} \quad \text{--- (5)}$$

Making rearrangements in Eq. (5) to calculate $t_{90\%}$ gives us,

$$t_{90\%} = t_{50\%}\left(\frac{0.9J_{max} - J_{min}}{0.1J_{max}}\right) \quad \text{--- (6)}$$

Similarly, in order to determine $t_{95\%}$ and $t_{99\%}$ from Eq. (4), we substitute respectively their current density values $J = 95\%J_{max}$ and $J = 99\%J_{max}$ in Eq. (4).

$$0.95J_{max} = (J_{max} - J_{min})\frac{t_{95\%}}{t_{50\%} + t_{95\%}} + J_{min} \quad \text{--- (7)}$$

$$0.99J_{max} = (J_{max} - J_{min})\frac{t_{99\%}}{t_{50\%} + t_{99\%}} + J_{min} \quad \text{--- (8)}$$

Solving Eqs. (7) and (8), $t_{95\%}$ and $t_{99\%}$ of an amperometric MG biosensor can be obtained as

$$t_{95\%} = t_{50\%}\left(\frac{0.95J_{max} - J_{min}}{0.05J_{max}}\right) \quad \text{--- (9)}$$

$$t_{99\%} = t_{50\%}\left(\frac{0.99J_{max} - J_{min}}{0.01J_{max}}\right) \quad \text{--- (10)}$$

2.6. Modified Hill model for the determination of response time

If the amperometry is performed at MG concentrations lower than the detection limit, amperometry will show a stable current density response. However, the current density response increases when the amount of added MG is higher than the limit of detection and finally inclined to a stable value at saturated MG concentration. In these conditions, amperometric curve follows sigmoidal behaviour. Hence Hill model is introduced in this work because it can explain the sigmoidal binding of MG biomolecules to the active sites on GLO 1 enzyme.

$$J = \frac{J_{max}[MG]^n}{K_M{}^n + [MG]^n} \quad \text{--- (11)}$$

where, n is the degree of co-operativity. Since the sigmoidal relationship between the current density and the concentration of MG adsorbing to the binding sites of GLO 1 is similar to the sigmoidal relationship between the current density and the incubation time, the MG concentration in Eq. (11) is replaced with time (t).

$$J = \frac{J_{max} t^n}{{t_{50\%}}^n + t^n} \quad \text{--- (12)}$$

where, $t_{50\%}$ is the 50% response time at which $J = \frac{J_{max}}{2}$. Even though current density response at $t = t_{max}$ is defined in the Eq. (12), current density response at $t = 0$ is not included. Hence J_{min} as an intercept is included in the Eq. (12).

$$J = \frac{J_{max} t^n}{{t_{50\%}}^n + t^n} + J_{min} \quad \text{--- (13)}$$

where, $t_{50\%}$ is the 50% response time at which $J = \frac{J_{max} + 2J_{min}}{2}$. But, the expected 50% response time is at $J = \frac{J_{max} - J_{min}}{2}$. Hence for the precise estimation of $t_{50\%}$ and J_{max}, the Eq. (12) is rewritten as,

$$J = (J_{max} - J_{min}) \frac{t^n}{{t_{50\%}}^n + t^n} + J_{min}, t_{min} \leq t \leq t_{max} \quad \text{--- (14)}$$

where, $t_{50\%}$ is the 50% response time at $J = \frac{J_{max} - J_{min}}{2}$. At $t = 0$, $J = J_{min}$. Similarly, at $t = t_{max}$, $J = (J_{max} - J_{min}) \frac{{t_{max}}^n}{{t_{50\%}}^n + {t_{max}}^n} + J_{min}$. In order to determine the 90%, 95% and 99% response time of MG biosensor, their corresponding amperometric current density response at 90%, 95% and 99% of its steady state value were calculated. Substituting $J = 90\% J_{max}$, $J = 95\% J_{max}$ and $J = 99\% J_{max}$ in Eq. (13), we get,

$$0.90 J_{max} = (J_{max} - J_{min}) \frac{{t_{90\%}}^n}{{t_{50\%}}^n + {t_{90\%}}^n} + J_{min} \quad \text{--- (15)}$$

$$0.95 J_{max} = (J_{max} - J_{min}) \frac{{t_{95\%}}^n}{{t_{50\%}}^n + {t_{95\%}}^n} + J_{min} \quad \text{--- (16)}$$

$$0.99 J_{max} = (J_{max} - J_{min}) \frac{{t_{99\%}}^n}{{t_{50\%}}^n + {t_{99\%}}^n} + J_{min} \quad \text{--- (17)}$$

Solving Eqs. (14), (15) and (16), $t_{90\%}$, $t_{95\%}$ and $t_{99\%}$ of an amperometric MG biosensor can be obtained as

$$t_{90\%} = t_{50\%}\left[\frac{0.90J_{max}-J_{min}}{0.10J_{max}}\right]^{1/n} \quad \text{--- (18)}$$

$$t_{95\%} = t_{50\%}\left[\frac{0.95J_{max}-J_{min}}{0.05J_{max}}\right]^{1/n} \quad \text{--- (19)}$$

$$t_{99\%} = t_{50\%}\left[\frac{0.99J_{max}-J_{min}}{0.01J_{max}}\right]^{1/n} \quad \text{--- (20)}$$

2.7. Measurement procedure for the determination of methylglyoxal in cow milk

Cow milk collected from local dairy farm (Thanjavur) was employed to assess the analytical performance of the calibrated linear models. 10 µL of cow milk sample was transferred to the electrochemical cell and the determination of MG was performed by amperometry using modified Pt working electrode. The MG content in cow milk was determined by using calibrated linear equations. All amperometric measurements were carried out by the standard addition method with three time measurements.

3. Results and discussion

3.1. Morphological characterization of nanostructured CeO_2 sample

As observed from the FE-SEM micrograph (Fig. 1(a)), CeO_2 particles were nearly spherical in shape. Particle size distribution of CeO_2 nanoparticles estimated from the selected FE-SEM micrograph is shown in Fig. 1(b). The diameter of the CeO_2 nanoparticles (n = 114) ranges from 125 nm to 172 nm with mean diameter of 149±23 nm.

3.2. Electrochemical behaviour of Pt/GLO 1/Chitosan and Pt/CeO_2/GLO 1/Chitosan bioelectrodes

Redox reaction of MG

Cyclic voltammograms of Pt/GLO 1/Chitosan and Pt/CeO_2/GLO 1/Chitosan bioelectrodes were performed in pH 7.4 PBS containing 1 µM of MG and GSH at a scan rate of 12 mVs^{-1} are shown in Fig. 1(c). Comparison of electrochemical parameters of various

modified Pt bioelectrodes is given in Table 1. The electrochemical responses of GLO 1 modified Pt bioelectrodes at various stages of fabrication towards MG were studied to understand the electrochemical reaction mechanism.

At first, Pt/GLO 1/Chitosan bioelectrode was tested in the potential range of -0.10 to -0.90 V. In the presence of GSH, this bioelectrode oxidized glutathione (GSH) to glutathione disulfide (GSSG) at -0.795 V. Further, GSSG reduced at -0.342 V to form reduced glutathione resulting in an effective electron transfer in the Pt/GLO 1/Chitosan bioelectrode. The electroactivity of GSH and GSSG[21] result in the reversible cyclic voltammetric response which in turn can be related to the redox nature of GSH biomolecule. In the presence of GSH and MG, GSH oxidized to GSSG at -0.679 V. The oxidized glutathione further reacted with MG at an applied potential of -0.764 V to form an intermediate product, hemithioacetal ($CH_3COCH(OH)$-SG), which further reacted with the active sites of GLO 1 enzyme to form the product namely S-D-lactoylglutathione ($CH_3CH(OH)CO$-SG) at an applied potential of -0.597 V. Similar electrochemical reaction mechanism was also observed at Pt/CeO_2/GLO 1/Chitosan nano-bioelectrode[22].

In presence of GSH

$$2GSH \leftrightharpoons GSSG + 2H^+ + 2e^-$$

In presence of GSH and MG

$$2GSH \rightarrow GSSG + 2H^+ + 2e^-$$

$$CH_3CCHO + GSSG + 2H^+ + 2e^- \rightarrow CH_3COCH(OH) - SG$$

$$CH_3COCH(OH) - SG + GLO\ 1 \rightarrow CH_3CH(OH)CO - SG$$

The oxidation and reduction reaction potentials of GSH biomolecule at the surface of Pt/GLO 1/Chitosan and Pt/CeO_2/GLO 1/Chitosan bioelectrodes were located at -0.795 V & -0.342 V and -0.810 V & -0.302 V respectively. The observed results are in good agreement with the previously reported redox potential of GSH biomolecule at the surface of Tris(2-

carboxyethyl)phosphine (TCEP) modified hanging mercury drop bioelectrode[23]. The reported E_{pa} and E_{pc} for the oxidation and reduction of GSH to GSSG and vice versa were -0.69 V and -0.44 V *vs Ag/AgCl* respectively.

In the presence of GSH and MG, the anodic and cathodic potentials of Pt/GLO 1/Chitosan and Pt/CeO_2/GLO 1/Chitosan bioelectrodes were observed at -0.679, -0.764, -0.597 V and -0.692, -0.771, -0.558 V respectively, which are the characteristic potentials of GSH: GSSG, MG: hemithioacetal and hemithioacetal: S-D-lactoylglutathione biomolecules. The observed anodic and cathodic potentials of various modified Pt bioelectrodes are in good accordance with the previously reported redox potentials of TCEP modified hanging mercury drop bioelectrode, SWNT/GCE and Pt/SWNT/GCE respectively[10,11,23].

3.3. Electron transfer properties of Pt/GLO 1/Chitosan and Pt/CeO_2/GLO 1/Chitosan bioelectrodes

Current density

There was no redox peak observed at bare Pt electrode, suggesting that bare Pt electrode was inactive in the applied potential range (see Table 1). The anodic and cathodic peak current densities observed at Pt/CeO_2/GLO 1/Chitosan nano-bioelectrode at -0.692 V, -0.771 V and -0.558 V were 1.79 - 3.03% larger than the current densities obtained at -0.679 V, -0.764 V and -0.597 V respectively using Pt/GLO 1/Chitosan bioelectrode. This indicated that CeO_2 nanoparticle can transfer enhanced number of electrons both in anodic and cathodic process.

Electron transfer rate constant

The electron transfer rate constant can be calculated using the following formula:

$$K_s = I_p/Q$$

where, I_p is the peak current and Q is the amount of charge consumed. In presence of GSH, K_s of GLO 1 enzyme immobilized on CeO_2 nanoparticle modified Pt electrode in the cathodic

and anodic process obtained at -0.692 V (K_s= 0.652 s^{-1}), -0.771 V (K_s=0.932 s^{-1}) and -0.558 V (K_s=0.214 s^{-1}) were 1.60 – 8.41% larger than that obtained at -0.679 V (K_s= 0.632 s^{-1}), -0.764 V (K_s= 0.917 s^{-1}) and -0.597 V (K_s= 0.196 s^{-1}) respectively for GLO 1 enzyme immobilized on Pt bioelectrode (see Table 1). This trend has confirmed that CeO_2 nanoparticles can enhance the rate of electron transfer in electrochemical process.

3.4. Amperometric measurements of the Pt/CeO_2/GLO 1/Chitosan and Pt/GLO 1/Chitosan bioelectrodes

There are two ways to determine MG concentration in cow milk samples either by measuring the production of hemithioacetal or by measuring the production of S-D-lactoylglutathione. Hence in this work, amperometric technique was employed for the reduction of MG to hemithioacetal and hemithioacetal to S-D-lactoylglutathione because it is more sensitive and provides less signal-to-noise ratio when compared to other electrochemical methods. Moreover, this method can help to detect MG in sample solution rapidly. Fig. 2 shows the amperometric current density responses of MG and hemithioacetal reduction on Pt/GLO 1/Chitosan and Pt/CeO_2/GLO 1/Chitosan bioelectrodes applied at a potential of (a) -0.764 & (b) -0.597 V and (c) -0.771 & (d) -0.558 V respectively for different concentrations of MG ranging from 5 to 50 μM. Well defined current density responses were observed for each successive addition of 5 μM MG. These results revealed the electrocatalytic behaviour of Pt/GLO 1/Chitosan and Pt/CeO_2/GLO 1/Chitosan bioelectrodes towards MG. The sensitivity of Pt/CeO_2/GLO 1/Chitosan and Pt/GLO 1/Chitosan bioelectrodes at -0.771, -0.558 V and -0.764, -0.597 V were determined as 2.868, 2.347 μA μM^{-1} and 2.125, 2.047 μA μM^{-1} respectively. Pt/CeO_2/GLO 1/Chitosan nano-bioelectrode showed maximum sensitivity towards MG at -0.771 V. Their corresponding detection limits (taken as 3.3σ/S, where, S is the sensitivity and σ is the standard deviation of the blank

signal) were 2.14, 3.65 nM and 10.73, 11.23 nM and the quantification limits (taken as 10σ/S) were 7.12, 12.51 nM and 35.73, 37.39 nM respectively.

3.5. Determination of response time and model validation

The modified Michaelis-Menten and Hill models were employed to calculate the response time ($t_{90\%}$, $t_{95\%}$ and $t_{99\%}$) of Pt/GLO 1/Chitosan and Pt/CeO_2/GLO 1/Chitosan bioelectrodes (Fig. 3 and 4). Parameters of these models for the determination of response time are given in Table 2. As can be seen from Table 2, a very fast response of MG and hemithioacetal reduction was observed at Pt/CeO_2/GLO 1/Chitosan nano-bioelectrode when the potential was applied at -0.771 and -0.558 V respectively. Response time of this electrode was lower than that of Pt/GLO 1/Chitosan bioelectrode.

The fit of modified Michaelis-Menten and Hill models can be evaluated using the adjusted regression coefficient (R^2)[24]. R^2 value of these models was greater than 99%, which indicated their ability to accurately predict the response time. Greater value of R^2 than 99% implied that the nonlinear models could explain more than 99% of the total variance. Relative prediction error (RPE) was calculated to assess the accuracy of modified Michaelis-Menten and Hill models. Modified Hill model showed good accuracy for Pt/CeO_2/GLO 1/Chitosan and Pt/GLO 1/Chitosan bioelectrodes. So it was chosen for response time measurement.

In order to detect the unknown concentration of MG in cow milk samples, calibration curves were established with the measured response time as dependent variable and the added MG concentration as independent variable. Fig. 5 shows the typical calibration curves of Pt/GLO 1/Chitosan (applied potential: (a) -0.764 V and (b) -0.597 V) and Pt/CeO_2/GLO 1/Chitosan nano-bioelectrodes (applied potential: (c) -0.771 V and (d) -0.558 V) in the determination of concentration of MG employing modified Hill model. The calibration plots showed a nonlinear relation between the response time and MG concentration. Response time

was increased with MG concentration with the nonlinear range from 5 to 50 μM. Their corresponding second-order polynomial fit equation is given in Table 3. The correlation coefficient (r) greater than 0.999 in all calibration plots showed the good precision of the proposed methods ($t_{90\%}$ *vs* [MG], $t_{95\%}$ *vs* [MG] and $t_{99\%}$ *vs* [MG]). Accuracy of the proposed method was assessed by calculating residual sum of squares (RSS). When compared with the accuracy results of $t_{95\%}$ *vs* [MG] and $t_{99\%}$ *vs* [MG] nonlinear models, only the $t_{90\%}$ *vs* [MG] nonlinear model showed low RSS value. This has indicated that $t_{90\%}$ *vs* [MG] nonlinear model can be employed for the accurate detection of MG in cow milk samples.

For Pt/GLO 1/Chitosan at -0.764 V,

$$t_{90\%}\,(s) = -8.960 \times 10^{-3}[\mathrm{MG}]^2(\mu\mathrm{M}^2) + 1.378\,[\mathrm{MG}](\mu\mathrm{M}) + 27.739 \quad \text{--- (21)}$$

For Pt/GLO 1/Chitosan at -0.597 V,

$$t_{90\%}\,(s) = -7.020 \times 10^{-3}[\mathrm{MG}]^2(\mu\mathrm{M}^2) + 1.350\,[\mathrm{MG}](\mu\mathrm{M}) + 43.230 \quad \text{--- (22)}$$

For Pt/CeO_2/GLO 1/Chitosan at -0.771 V,

$$t_{90\%}\,(s) = -6.150 \times 10^{-3}[\mathrm{MG}]^2(\mu\mathrm{M}^2) + 0.803\,[\mathrm{MG}](\mu\mathrm{M}) + 13.179 \quad \text{--- (23)}$$

For Pt/CeO_2/GLO 1/Chitosan at -0.558 V,

$$t_{90\%}\,(s) = -3.070 \times 10^{-3}[\mathrm{MG}]^2(\mu\mathrm{M}^2) + 0.675\,[\mathrm{MG}](\mu\mathrm{M}) + 12.866 \quad \text{--- (24)}$$

3.6. Reproducibility, repeatability and stability of the Pt/CeO_2/GLO 1/Chitosan and Pt/GLO 1/Chitosan bioelectrodes

For the reproducibility and repeatability, 10 different fabricated Pt/CeO_2/GLO 1/Chitosan and Pt/GLO 1/Chitosan bioelectrodes were used for the reduction of MG and hemithioacetal at an optimized potential. All the electrochemical analyses using the two electrodes were individually performed in the presence of 1 μM of MG and GSH in 0.1 M PBS (pH 7.4). And their results were employed to estimate relative standard deviation (RSD). The Pt/CeO_2/GLO 1/Chitosan and Pt/GLO 1/Chitosan bioelectrodes at -0.771, -0.558 V and

-0.764, -0.597 V achieved satisfactory reproducibility with the RSD of 1.02%, 1.034% and 1.87%, 1.54% respectively. RSD values of 0.54, 0.63% and 0.96, 0.87% indicated the good repeatability of the proposed Pt/CeO_2/GLO 1/Chitosan nano-bioelectrode at -0.771 V.

To assess the storage stability of Pt/CeO_2/GLO 1/Chitosan and Pt/GLO 1/Chitosan bioelectrodes, their current density response to detect 5 μM MG was monitored every day for 20 days. The Pt/CeO_2/GLO 1/Chitosan and Pt/GLO 1/Chitosan bioelectrodes operated at -0.771, -0.558 V and -0.764, -0.597 V were retained 98% of its initial response even after 20 days of storage period, which depicted the good stability of the Pt/CeO_2/GLO 1/Chitosan bioelectrode. These results also implied that CeO_2 nanoparticles provided a biocompatible environment for the immobilized GLO 1 enzyme.

3.7. Interference study and detection of MG in cow milk samples

Enzymes possess a tendency to interact with metal ions. As well as, cow milk contains many compounds which may interfere or block the interaction between the GLO 1 and MG. So, interference study was performed by considering 0.1 mM of possible interferents namely, Ni^{2+}, Cd^{2+}, Zn^{2+}, Cu^{2+}, urea, sucrose, ascorbic acid and lactic acid at an applied potential of -0.771, -0.558 V and -0.764, -0.597 V using Pt/CeO_2/GLO 1/Chitosan and Pt/GLO 1/Chitosan bioelectrodes respectively. Upon the addition of 5 μM MG to 0.1 M PBS (pH 7.4), a clear current density response was observed. After addition of 5 μM MG to the electrochemical cell again, the Pt/CeO_2/GLO 1/Chitosan and Pt/GLO 1/Chitosan bioelectrodes responses were almost close to the current density observed in the absence of interferents, manifesting the good selectivity of the proposed bioelectrodes.

The cow milk samples were collected from local dairy farm without any sample pretreatment. The MG level estimated using Pt/GLO 1/Chitosan bioelectrode at -0.764, -0.597 V were determined to be 12.63, 12.64 μM, which was close to the estimated value of 12.66 μM obtained by Pt/CeO_2/GLO 1/Chitosan nano-bioelectrode. The recovery values of

MG in spiked cow milk samples were in the range of 99.21-101.72, 98.64-102.75% and 97.32-102.28, 96.82-103.92% for Pt/CeO_2/GLO 1/Chitosan and Pt/GLO 1/Chitosan bioelectrodes at optimized potentials (Table 4), signifying the developed MG biosensor had the ability to overcome potential interferents .

The analytical performance of Pt/CeO_2/GLO 1/Chitosan and Pt/GLO 1/Chitosan bioelectrodes were compared to that of other reported MG biosensors with nano-interface. The Pt/CeO_2/GLO 1/Chitosan at an applied potential of -0.771 V showed an excellent detection limit which is the lowest of those summarized in Table 5 and comparable to that obtained with ZnO nanoflakes, ZnO nanosepals, SWCNT and SWCNT-Pt nanoparticles modified electrodes. Table 5 shows the analytical parameters of Pt/CeO_2/GLO 1/Chitosan. Even though the MG biosensors constructed by immobilizing SWCNT, SWCNT-Pt on GCE electrode showed extended linear range than the Pt/CeO_2/GLO 1/Chitosan nano-bioelectrode, it should be noted that only the proposed bioelectrode could accurately detect nanomolar concentrations of MG with a good precision.

4. Conclusion

An electrochemical biosensor for the specific detection of MG in cow milk was successfully demonstrated. Very interestingly, GSH and Pt/CeO_2/GLO 1/Chitosan nano-bioelectrode showed electrocatalytic ability toward the oxidation of MG to hemithioacetal and reduction of hemithioacetal to S-D-lactoylglutathione respectively. The specific and rapid detection of MG were achieved by utilizing GLO 1 enzyme and CeO_2 nano-interface immobilized on the surface of Pt working electrode. The developed bioelectrode showed the enhanced electron transport between the immobilized GLO 1 enzyme and Pt electrode through the CeO_2 nanoparticle as the nanoscale connector. The amperometric Pt/CeO_2/GLO 1/Chitosan biosensor coupled with the modified Michaelis-Menten/Hill model can predict the response time with high accuracy. The experiments in cow milk samples manifested the

feasibility of the developed MG biosensor in complex matrix. The good sensitivity, repeatability, reproducibility and recovery obtained with the Pt/CeO_2/GLO 1/Chitosan nano-bioelectrode demonstrated that it could be used as promising MG biosensor. The work could be extended towards the detection of MG in other food products prepared by roasting, grilling and broiling at very high temperatures.

Acknowledgements

The authors are grateful to the Department of Science & Technology, New Delhi, for their financial support (DST/TM/WTI/2K14/197(a)(G)), DST/TSG/PT/2008/28, SR/FST/ETI-284/2011(C) and (Nano Mission Council (No. SR/NM/PG-16/2007)). The research was supported by Professor T. R. Rajagopalan research fund, SASTRA University. We also acknowledge SASTRA University, Thanjavur for extending infrastructural support to carry out the study.

References

1 T. Bose, A. Bhattacherjee, S. Banerjee and A. S. Chakraborti, *Arch. Biochem. Biophys.*, 2013, **529**, 99–104.

2 J. Uribarri, S. Woodruff, S. Goodman, W. Cai, X. Chen, R. Pyzik, A. Yong, G. E. Striker and H. Vlassara, *J. Am. Diet. Assoc.*, 2010, **110**, 911–916.e12.

3 M. P. Kalapos, *Diabetes Res. Clin. Pract.*, 2013, **99**, 260–271.

4 D. Tan, Y. Wang, C. Y. Lo and C. T. Ho, *Asia Pac. J. Clin. Nutr.*, 2008, **17**, 261–264.

5 Y. Wang and C.-T. Ho, *Chem. Soc. Rev.*, 2012, **41**, 4140.

6 T. Goldberg, W. Cai, M. Peppa, V. Dardaine, B. S. Baliga, J. Uribarri and H. Vlassara, *J. Am. Diet. Assoc.*, 2004, **104**, 1287–1291.

7 A. J. Kandhro, M. A. Mirza and M. Y. Khuhawar, *J. Chromatogr. Sci.*, 2008, **46**, 539–43.

8 B. G. Chen, C. H. Lin, C. Chen, B. Hambsch and C.-L. Chern, *Chromatographia*, 2013, **76**, 571–576.

9 M. A. Mirza, A. J. Kandhro, M. Y. Khuhawar, R. Arain, M. A. Choudhary and T. M. Jahangir, *J. Chem. Soc. Pakistan*, 2013, **35**, 52–57.

10 S. Chatterjee and A. Chen, *Anal. Chim. Acta*, 2012, **751**, 66–70.

11 S. Chatterjee, J. Wen and A. Chen, *Biosens. Bioelectron.*, 2013, **42**, 349–354.

12 A. Thangavel, S. Alagesan, N. Nesakumar, B. L. Ramachandra, M. B. Gumpu, S. Vedantham, S. Sethuraman, U. M. Krishnan and J. B. B. Rayappan, *Sens. Lett.*, 2015, **13**, 328–337.

13 M. Ezhilan, S. Alagesan, B. L. Ramachandra, M. B. Gumpu, N. Nesakumar, S. Vedantham, S. Sethuraman, U. M. Krishnan and J. B. B. Rayappan, *Sens. Lett.*, 2015, **13**, 245–253.

14 D. Grieshaber, R. MacKenzie, J. Vörös and E. Reimhult, *Sensors*, 2008, **8**, 1400–1458.

15 M. Pumera, S. Sánchez, I. Ichinose and J. Tang, *Sensors Actuators B Chem.*, 2007, **123**, 1195–1205.

16 D. Patil, N. Q. Dung, H. Jung, S. Y. Ahn, D. M. Jang and D. Kim, *Biosens. Bioelectron.*, 2012, **31**, 176–181.

17 P. R. Solanki, A. Kaushik, V. V Agrawal and B. D. Malhotra, *NPG Asia Mater.*, 2011, **3**, 17–24.

18 P. R. Solanki, C. Dhand, A. Kaushik, A. A. Ansari, K. N. Sood and B. D. Malhotra, *Sensors Actuators B* , 2009, **141**, 551–556.

19 N. Nesakumar, S. Sethuraman, U. M. Krishnan and J. B. B. Rayappan, *J. Colloid Interface Sci.*, 2013, **410**, 158–164.

20 J. L. Montañez-Soto, S. Alegret, J. A. Salazar-Montoya and E. G. Ramos-Ramírez, *Eur. Food Res. Technol.*, 2006, **223**, 379–386.

21 J. P. H. Stephen A. Wring, *Analyst*, 1989, **114**, 1563–1570.

22 P. J. Thornalley, *Biochem. J.*, 1990, **269**, 1–11.

23 R. Kizek, J. Vacek, L. Trnková and F. Jelen, *Bioelectrochemistry*, 2004, **63**, 19–24.

24 M. Asadollahi-Baboli and a. Mani-Varnosfaderani, *Measurement*, 2014, **47**, 145–149.

List of Figures

Fig. 1. (a) FE-SEM image of the as-prepared CeO_2 nanoparticles, (b) distribution of the CeO_2 nanoparticle's diameter and cyclic voltammograms of (c) Pt/GLO 1/Chitosan and (d) Pt/CeO_2/GLO 1/Chitosan bioelectrodes in 0.1 M PBS (7.4 pH) containing 1.0 μM of methylglyoxal and GSH at 12 mV/s.

Fig. 2. Amperometric current density responses at Pt/GLO 1/Chitosan and Pt/CeO_2/GLO 1/Chitosan bioelectrodes applied at a potential of (a) -0.764 and (b) -0.597 V and (c) -0.771 and (d) -0.558 V respectively in 0.1 M PBS (pH 7.4) containing 50 μM GSH.

Fig. 3. Modified Michaelis-Menten curves using Pt/GLO 1/Chitosan bioelectrode upon successive addition of 5 μM methylglyoxal at an applied potential of (a) -0.764 and (c) -0.597 V and Hill curves using Pt/GLO 1/Chitosan bioelectrode upon successive addition of 5 μM methylglyoxal at an applied potential of (b) -0.764 and (d) -0.597 V.

Fig. 4. Modified Michaelis-Menten curves using Pt/CeO_2/GLO 1/Chitosan bioelectrode upon successive addition of 5 μM methylglyoxal at an applied potential of (a) -0.771 and (c) -0.558 V and Hill curves using Pt/CeO_2/GLO 1/Chitosan bioelectrode upon successive addition of 5 μM methylglyoxal at an applied potential of (b) -0.771 and (d) -0.558 V.

Fig. 5. Typical calibration curves of Pt/GLO 1/Chitosan bioelectrode (applied potential: (a) -0.764 V and (b) -0.597 V) and Pt/CeO_2/GLO 1/Chitosan bioelectrode (applied potential: (c) -0.771 V and (d) -0.558 V) in the determination of concentration of methylglyoxal.

Fig. 1. (a) FE-SEM image of the as-prepared CeO_2 nanoparticles, (b) distribution of the CeO_2 nanoparticle's diameter and cyclic voltammograms of (c) Pt/GLO 1/Chitosan and (d) Pt/CeO_2/GLO 1/Chitosan bioelectrodes in 0.1 M PBS (7.4 pH) containing 1.0 µM of methylglyoxal and GSH at 12 mV/s.

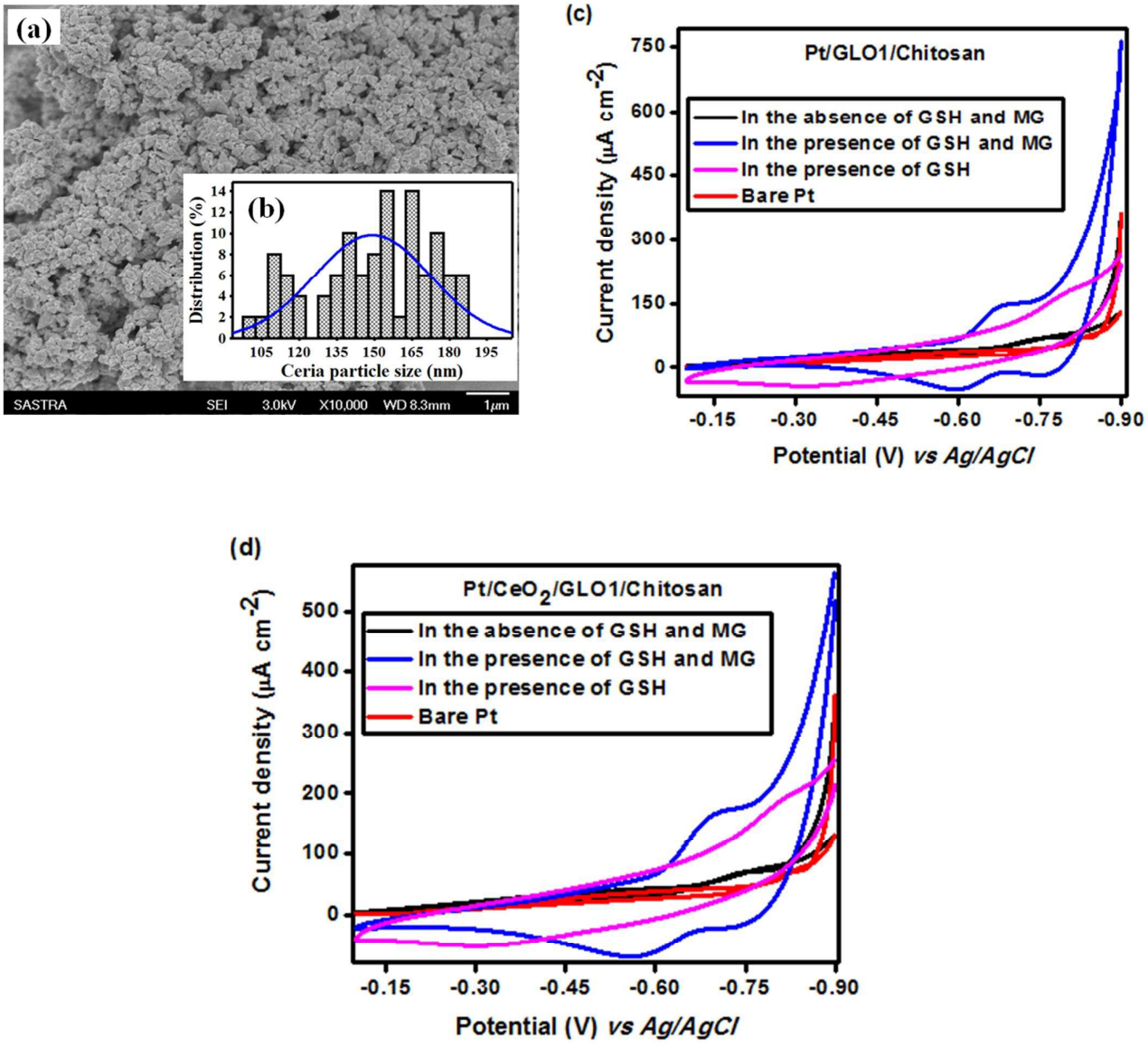

Fig. 2. Amperometric current density responses at Pt/GLO 1/Chitosan and Pt/CeO_2/GLO 1/Chitosan bioelectrodes applied at a potential of (a) -0.764 & (b) -0.597 V and (c) -0.771 & (d) -0.558 V respectively in 0.1 M PBS (pH 7.4) containing 50 µM GSH.

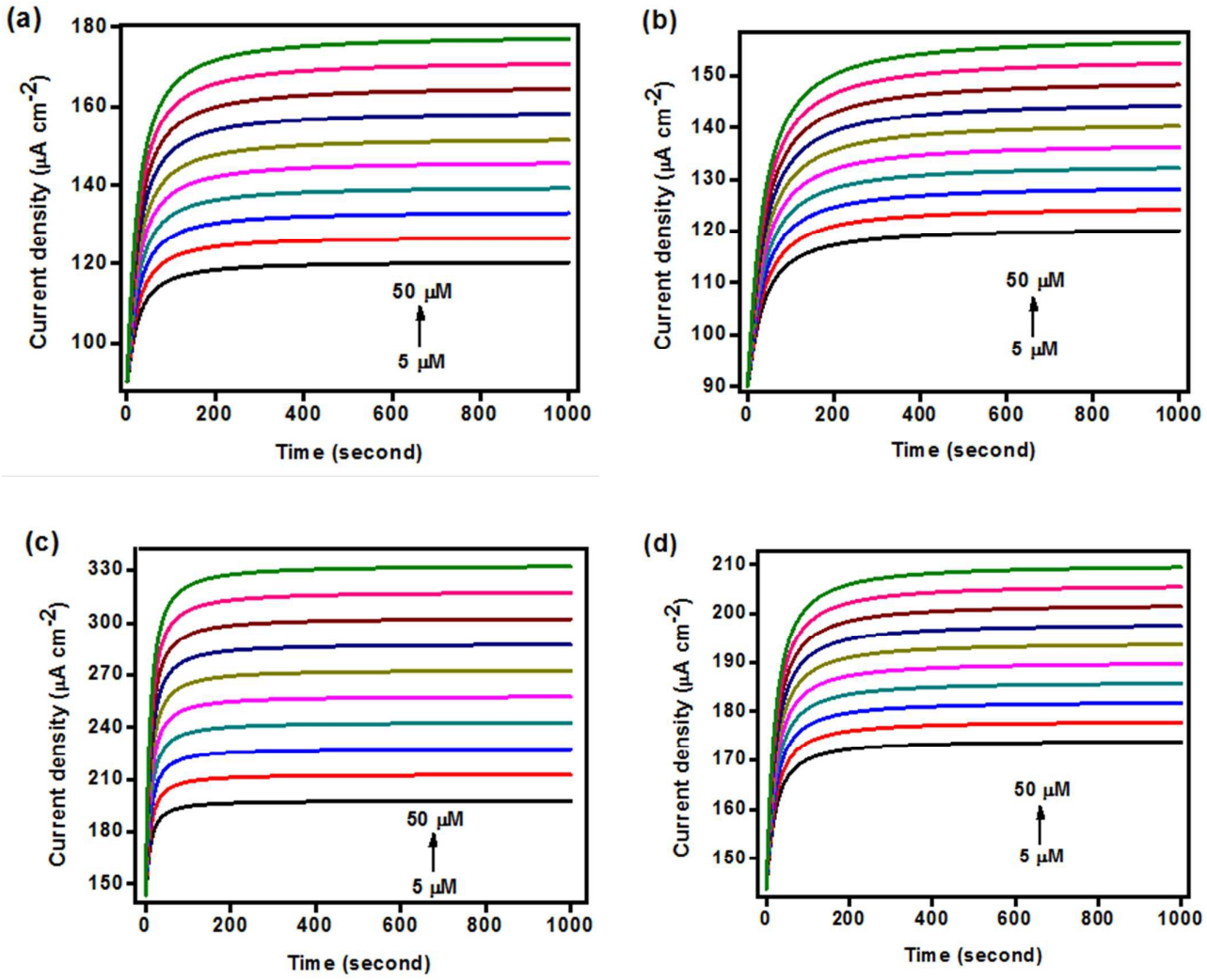

Fig. 3. Modified Michaelis-Menten curves using Pt/GLO 1/Chitosan bioelectrode upon successive addition of 5 µM methylglyoxal at an applied potential of (a) -0.764 and (c) -0.597 V and Hill curves using Pt/GLO 1/Chitosan bioelectrode upon successive addition of 5 µM methylglyoxal at an applied potential of (b) -0.764 and (d) -0.597 V.

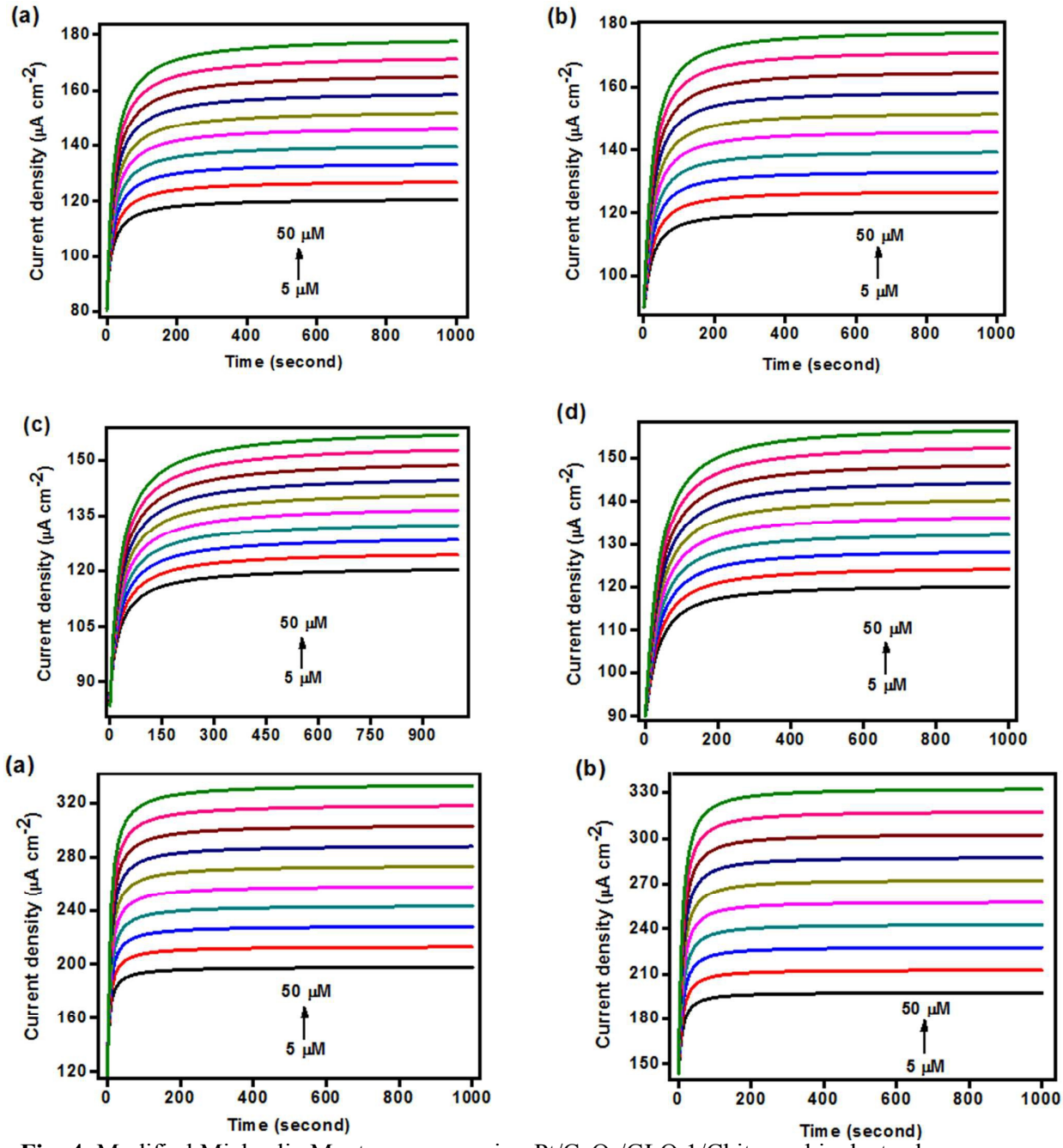

Fig. 4. Modified Michaelis-Menten curves using Pt/CeO_2/GLO 1/Chitosan bioelectrode upon successive addition of 5 µM methylglyoxal at an applied potential of (a) -0.771 and (c) -0.558

V and Hill curves using Pt/CeO_2/GLO 1/Chitosan bioelectrode upon successive addition of 5 µM methylglyoxal at an applied potential of (b) -0.771 and (d) -0.558 V.

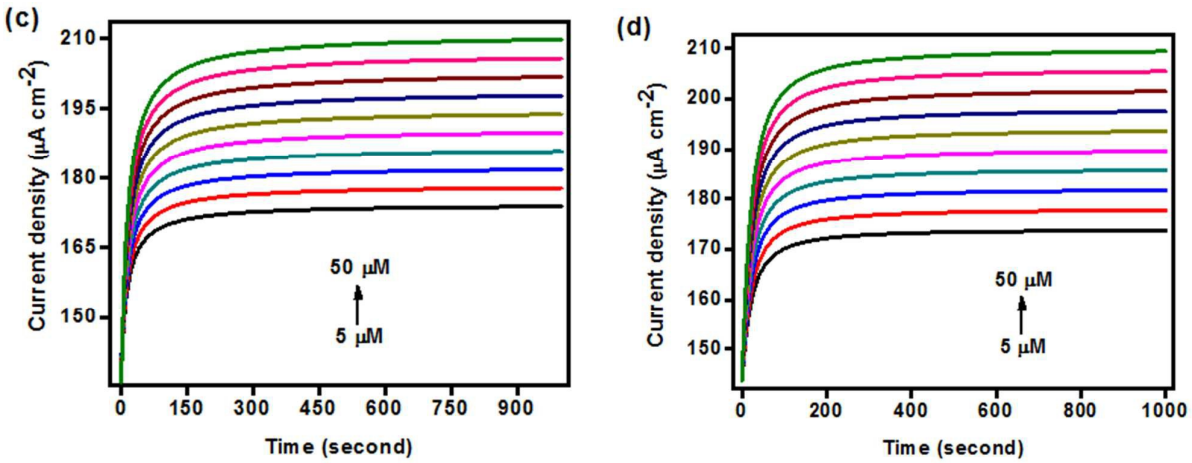

Fig. 5. Typical calibration curves of Pt/GLO 1/Chitosan bioelectrode (applied potential: (a) -0.764 V and (b) -0.597 V) and Pt/CeO_2/GLO 1/Chitosan bioelectrode (applied potential: (c) -0.771 V and (d) -0.558 V) in the determination of concentration of methylglyoxal.

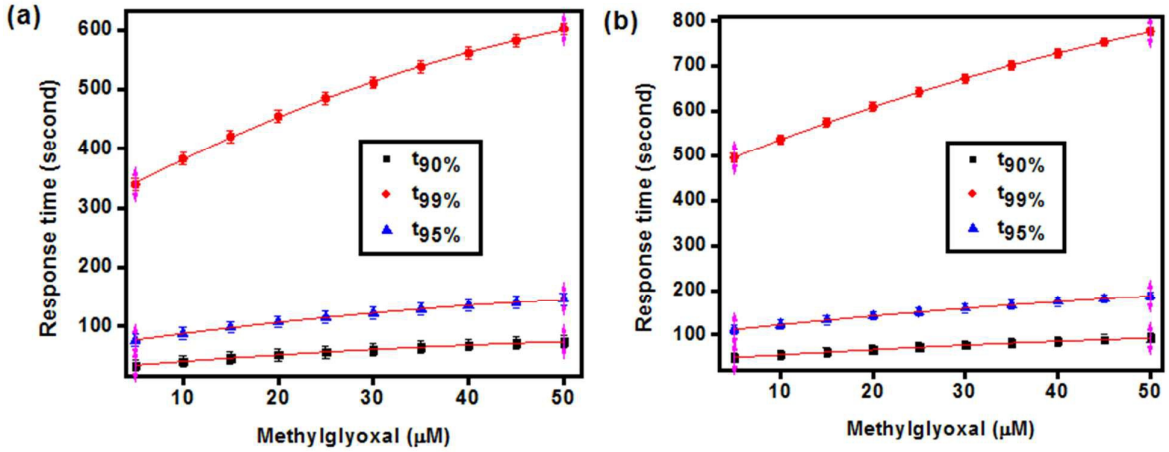

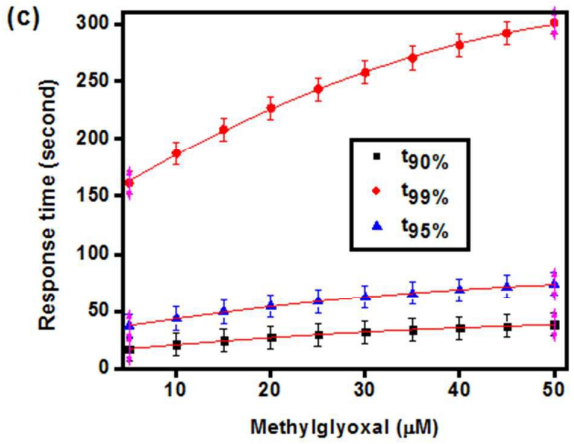

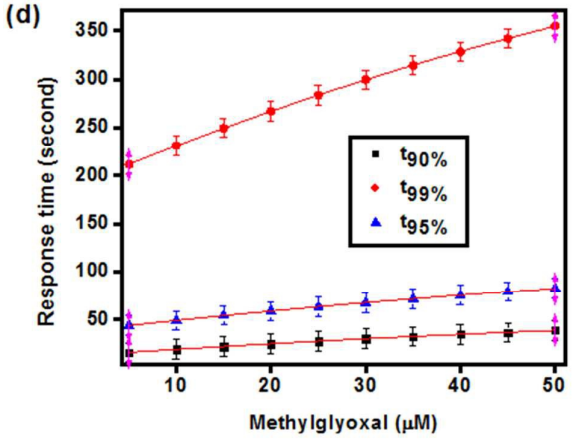

List of Tables

Table 1. Electrochemical parameters of different modified electrodes.

Table 2. Parameters of modified Michaelis-Menten and Hill models for the determination of response time.

Table 3. Parameters of second order polynomial model for the determination of methylglyoxal.

Table 4. Determination results of methylglyoxal in cow milk samples (n=3).

Table 5. Comparison of analytical parameters of the developed methylglyoxal biosensor with the previously reported biosensor for methylglyoxal determination.

Table 1. Electrochemical parameters of different modified electrodes.

Electrode		E_p (V)	J_p ($\mu A\ cm^{-2}$)	K_s (s^{-1})
Pt/GLO 1/Chitosan	in presence of GSH	-0.795	44.013	0.263
		-0.342	43.121	0.251
	in presence of GSH+ MG	-0.679	92.197	0.632
		-0.764	126.178	0.917
		-0.597	38.344	0.196
Pt/CeO_2/GLO 1/Chitosan	in presence of GSH	-0.810	45.096	0.274
		-0.302	44.745	0.269
	in presence of GSH+ MG	-0.692	95.064	0.652
		-0.771	130.127	0.932
		-0.558	39.045	0.214

Table 2. Parameters of modified Michaelis Menten and Hill models for the determination of response time.

Electrode	Model	Applied potential (V)	Detection range (µM)	$t_{99\%}$ (s)	$t_{95\%}$ (s)	$t_{90\%}$ (s)	$t_{50\%}$ (s)	RPE	R^2
Pt/GLO 1/ Chitosan	Modified Michaelis-Menten	-0.764	5-50	507.453-1002.328	86.677-185.652	34.080-83.568	18.515	0.055	0.996
	Modified Hill	-0.764	5-50	339.700-601.745	76.589-146.595	34.015-74.516	23.76	0.002	0.999
	Modified Michaelis-Menten	-0.597	5-50	764.942-1306.380	130.494-238.782	51.188-105.332	28.117	0.059	0.997
	Modified Hill	-0.597	5-50	495.396-777.016	111.692-187.060	49.606-93.336	34.65	0.001	0.999
Pt/CeO_2/ GLO 1/ Chitosan	Modified Michaelis-Menten	-0.771	5-50	229.387-483.015	39.829-90.555	16.134-41.497	7.559	0.147	0.994
	Modified Hill	-0.771	5-50	161.144-300.862	36.781-74.021	16.729-38.191	10.554	0.001	0.999
	Modified Michaelis-Menten	-0.558	5-50	293.598-543.507	46.094-96.076	15.156-40.147	15.781	0.053	0.996
	Modified Hill	-0.558	5-50	211.696-355.050	43.931-82.697	16.078-39.035	20.557	0.001	0.999

Table 3. Parameters of second order polynomial model for the determination of methylglyoxal.

Electrode	Parameter	$t_{90\%}$ vs [MG]	$t_{95\%}$ vs [MG]	$t_{99\%}$ vs [MG]
Pt/GLO 1/Chitosan @-0.764 V	sample number	10	10	10
	range (μM)	5-50	5-50	5-50
	β_2	-8.96×10^{-3}	-1.51×10^{-2}	-5.564×10^{-2}
	β_1	1.378	2.362	8.798
	β_0	27.739	65.779	299.335
	RSS*	0.631	1.655	21.508
	r	0.999	0.999	0.999
Pt/GLO 1/Chitosan @-0.597 V	sample number	10	10	10
	range (μM)	5-50	5-50	5-50
	β_2	-7.02×10^{-3}	-1.172×10^{-2}	-4.293×10^{-2}
	β_1	1.35	2.306	8.574
	β_0	43.230	100.759	454.674
	RSS*	0.162	0.396	4.938
	r	0.999	0.999	0.999
Pt/CeO_2/GLO 1/ Chitosan @- 0.771 V	sample number	10	10	10
	range (μM)	5-50	5-50	5-50
	β_2	-6.15×10^{-3}	-1.05×10^{-2}	-3.896×10^{-2}
	β_1	0.803	1.384	5.174
	β_0	13.179	30.631	138.100
	RSS*	0.370	1.008	13.344
	r	0.999	0.999	0.999
Pt/CeO_2/GLO 1/ Chitosan @-0.558 V	sample number	10	10	10
	range (μM)	5-50	5-50	5-50
	β_2	-3.07×10^{-3}	-4.75×10^{-3}	-1.683×10^{-2}
	β_1	0.675	1.118	4.096
	β_0	12.866	38.569	191.985
	RSS*	0.031	0.050	0.526
	r	0.999	0.999	0.999

Table 4. Determination results of methylglyoxal in cow milk samples (n=3).

MG spiked	Pt/GLO 1/Chitosan at -0.764 V		Pt/GLO 1/Chitosan at -0.597 V		Pt/CeO_2/GLO 1/ Chitosan at -0.771 V		Pt/GLO 1/CeO_2/ Chitosan at -0.558 V	
	MG detected	Recovery	MG detected	Recovery	MG detected	Recovery	MG detected	Recovery
(µM)	(µM)	(%)	(µM)	(%)	(µM)	(%)	(µM)	(%)
0	12.630	---	12.640	---	12.660	---	12.660	---
0.2	12.825	97.320	12.834	96.820	12.860	99.750	12.860	99.860
0.4	13.035	101.320	13.056	103.920	13.067	101.720	13.062	100.580
0.6	13.244	102.280	13.24	99.980	13.255	99.210	13.252	98.640
0.8	13.426	99.560	13.418	97.240	13.456	99.540	13.482	102.750
1.0	13.614	98.430	13.654	101.360	13.665	100.480	13.671	101.090

Table 5. Comparison of analytical parameters of the developed methylglyoxal biosensor with the previously reported biosensor for methylglyoxal determination.

Parameters	Electrode matrix							
	Pt/GLO 1/Chitosan		Pt/CeO_2/GLO 1/Chitosan		GCE/SWCNT/ Pt	GCE/SWCNT	Pt/ZnO/GLO 1/Chitosan	Pt/ZnO/GLO 1/Chitosan
Applied potential (V *vs Ag/AgCl*)	-0.764	-0.597	-0.771	-0.558	-0.760	-0.844	-0.470	-0.400
Sample	Cow milk	Cow milk	Cow milk	Cow milk	Beer/wine	Human plasma	Human blood	Grilled chicken
Technique	Amperometry	Amperometry	Amperometry	Amperometry	Square wave voltammetry	Square wave voltammetry	Linear sweep voltammetry	Linear sweep voltammetry
Nanomaterial	Not used	Not used	CeO_2	CeO_2	SWCNT-Pt	SWCNT	ZnO sepals	ZnO flakes
Enzyme	GLO 1	GLO 1	GLO 1	GLO 1	Not used	Not used	GLO 1	GLO 1
Range of detection (µM)	5 - 50	5 - 50	5 - 50	5 - 50	0.1 - 100	0.1 - 100	0.2 - 100	0.2 – 100
Sensitivity (µA μM^{-1})	2.125	2.047	2.868	2.347	0.114	0.076	0.022	2.615
Repeatability (%RSD)	0.96	0.87	0.54	0.63	1.52	1.83	0.582	1.167
Reproducibility (%RSD)	1.87	1.54	1.02	1.34	1.95	2.76	6.547	5.564
LOD (nM)	10.73	11.23	2.14	3.65	2.80	---	---	---
LOQ (nM)	35.730	37.396	7.126	12.514	9.24	---	---	---
Accuracy (%RPE)	0.2	0.1	0.1	0.1	---	---	0.191	0.573
Stability (days)	20 (98%)	20 (98%)	20 (98%)	20 (98%)	45 (90%)	20 (96%)	---	---
Inhibition (%)	2.69	3.14	2.67	3.12	4.21	4.67	---	---
Response time (s)	< 75	< 94	< 39	< 40	---	---	---	---
Recovery (%)	97.32-102.28	96.82-103.92	99.21-101.72	98.64-102.75	95.04-104.74	95.01-104.56	91.15-116.488	95.895-108.191
Reference	Present work	Present work	Present work	Present work	[10]	[11]	[12]	[13]

Graphical Abstract